HHS Public Access

Author manuscript

ACS Infect Dis. Author manuscript; available in PMC 2019 December 14.

Published in final edited form as:

ACS Infect Dis. 2019 June 14; 5(6): 974–981. doi:10.1021/acsinfecdis.9b00039.

Synthesis and Evaluation of QS-7-Based Vaccine Adjuvants

Pengfei Wang[*,†], **Đani Škalamera**[†], **Xianwei Sui**[†], **Ping Zhang**[*,‡], **Suzanne M. Michalek**[§]

[†]Department of Chemistry, University of Alabama at Birmingham, 901 14th Street South, Birmingham, Alabama 35294, United States

[‡]Department of Pediatric Dentistry, University of Alabama at Birmingham, 901 14th Street South, Birmingham, Alabama 35294, United States

[§]Department of Microbiology, University of Alabama at Birmingham, 901 14th Street South, Birmingham, Alabama 35294, United States

Abstract

We have designed and synthesized two analogs (5 and 6) of QS-7, a natural saponin compound isolated from *Quillaja saponaria* (QS) Molina tree bark. The only structural difference between compound 5 and 6 is that 5 is acetylated at the 3- and 4-O positions of the quillaic acid C28 fucosyl unit while 6 is not. However, the two analogs show significantly different immunostimulant profiles. Compound 5 may potentiate a mixed Th1/Th2 (Th, T helper cells) immune response against the specific antigens while compound 6 may only induce a Th2-biased immunity. These results suggest that the 3- and/or 4-O acetyl groups of the fucosyl unit may play an important role in tuning the adjuvanticity of the QS-7 analogs, and compound 5 can serve as a structurally defined synthetic adjuvant when a mixed Th1/Th2 immune responses is desired.

Graphical Abstract

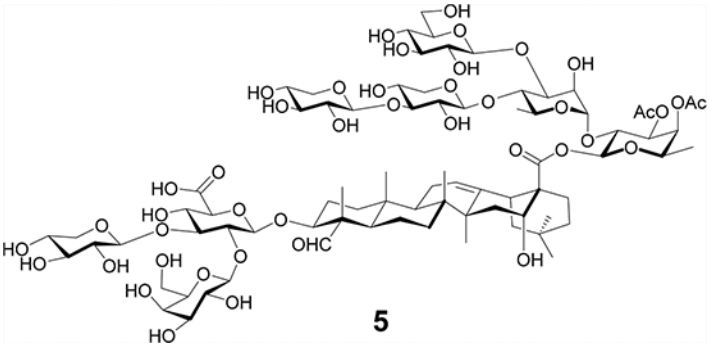

Keywords

vaccine; adjuvant; immunostimulant; saponin; QS-7

[*]Corresponding Authors: Phone: (205)996-5625. wangp@uab.edu (P.W.). Phone: (205)996-9803. pingz@uab.edu (P.Z.).

Supporting Information

The Supporting Information is available free of charge on the ACS Publications website at DOI: 10.1021/acsinfecdis.9b00039.

Serum IgG, IgG1, and IgG2a data, mice body weight data and graph, and ^{1}H NMR spectra of the new compounds **5** and **6** (PDF)

The authors declare no competing financial interest.

Vaccine adjuvant is a substance formulated as part of a vaccine boost and/or modulates the antigen-specific immune responses. Many different types of adjuvants have been tested in clinical trials,[1–4] but only a few are approved for human use. The U.S. Food and Drug Administration (FDA) recently approved QS-21 as a component of the GlaxoSmithKline's (GSK) AS01b adjuvant formulation for the human vaccine Shingrix. QS-21 (**1** and **2**, Figure 1) has a favorable adjuvant activity profile, potentiating a balanced Th1/Th2 (Th, T helper cells) response with antigen-specific cytotoxic T cell (CTL) production.[5,6] QS-21 is a mixture of two isomeric saponins extracted from the tree bark of *Quillaja saponaria* (QS) Molina, and the two isomers, QS-21_{api} (**1**) and QS-21_{xyl} (**2**), have the same adjuvanticity and toxicity. Their structures only differ in the terminal sugar unit of the linear tetrasaccharide that connects to the C28 carboxyl group of the quillaic acid triterpene core. QS-21_{api} (1) has a β-D-apiofuranosyl (api) unit, and QS-21_{xyl} (2) has a β-D-xylopyranosyl (xyl) unit; they are in a 2:1 ratio. A chiral and glycosylated fatty acyl chain is connected to the C4 hydroxyl group of the fucosyl unit in the tetrasaccharide, and at the C3 hydroxyl group of the quillaic acid core, there is a branched trisaccharide connecting through a β-glycosidic linkage. QS-21 has been studied in over one hundred clinical trials of vaccines against cancers and infectious diseases;[7,8] however, it has its own drawbacks including chemical instability, dose-limiting toxicity, limited supply, and laborious and low-yielding purification. Significant efforts have been devoted to developing synthetic analogs of QS-21 to overcome the limitations of the natural product.[9–16]

In addition to QS-21, other structurally identified QS saponins can also serve as promising leads in developing new QS saponin-based synthetic immunostimulants with improved adjuvant activity and accessibility and reduced toxicity.[17] For example, QS-7 (**3** and **4**, Figure 1), an underexplored member of the QS family of saponins, has adjuvant activity similar to that of QS-21, i.e., inducing a balanced Th1/Th2 response with a strong CD8+ (cluster of differentiation 8) CTL production.[5,18,19] Interestingly, its structure is distinctively different from that of QS-21 (Figure 1). It lacks QS-21's characteristic long chiral acyl side chain at the 4-O position of the fucopyranosyl unit that connects to the C28 carboxyl group of quillaic acid; instead, it has a small acetyl at the 4-O position. In addition, it has two extra monosaccharide units in the C28 oligosaccharide domain compared with QS-21; thus, it is more hydrophilic than QS-21. QS-7 has similar immune stimulating ability as QS-21, but it is less hemolytic and lethal than QS-21,[18] which makes it an attractive lead in the development of improved QS saponin-based vaccine adjuvants.

Herein, we report our synthesis and evaluation of QS-7 analogs **5** and **6** (Figure 2). Analog **5** replaces the α-L-rhamnopyranosyl (rha) unit at the 3-O position of the C28 fucopyranosyl unit in natural QS-7_{xyl} (4) with a simple acetyl group. Earlier studies of QS-21 reveal that its 4-O acyl side chain migrates to the neighboring 3-O position through transesterification in solution, resulting in a regioisomer of similar adjuvant activity,[20] which suggests that acetylation at 3-O or 4-O position may have a similar biological effect.[21] It will be interesting to see how adjuvant activity will be affected when both sites are acetylated. Moreover, analog **5** is more synthetically accessible than the analog with a 3-OH/4-OAc (Ac, acetyl) combination. To evaluate the impact of the acetyl groups in **5** on its adjuvant activity, we also prepared analog **6** without the two acetyl groups for comparison.

RESULTS AND DISCUSSION

To synthesize **5** and **6**, we would first synthesize the branched pentasaccharide portion of the molecules by using the two-stage allyl-glycoside-donor-activation approach.[22–25] With this approach, the anomeric allyl group of a glycosyl donor was first isomerized to a prop-1-enyl group by using the hydrogen-activated catalyst $[Ir(COD)(PMePh_2)_2]PF_6$[26, 27] (COD, cyclo-octadiene; P, phosphine; Me, methyl; Ph, phenyl; F, fluoro) or by using potassium *tert*-butyloxide.[28] Subsequent treatment of the obtained prop-1-enyl donor with *N*-iodosuccinimide (NIS)/triflic acid (TfOH) in the presence of an allyl glycosyl acceptor provided the desired glycosylic bond. We prepared allyl monosaccharide building blocks **7**–**11** (Scheme 1).[17] By repeatedly using the two-stage allyl-glycoside-donor-activation approach and proper protecting group manipulations, we assembled these monosaccharide building blocks into pentassachride **12**. Currently, this two-stage allyl-glycoside-donor-activation approach is not optimized for a carboxyl acceptor; thus, we converted pentasccharide **12** into its corresponding trichloroacetimidate donor. Glycosylation of the known quillaic acid-trisaccharide conjugate (**13**) with the imidate donor provided fully protected saponin skeleton **14**.[17] The subsequent global deprotection began with removal of all the benzyl groups under hydrogenolysis conditions to provide intermediate **15**. Removal of the remaining triethylsilyl (TES) groups was carried out with trifluoroacetic acid (TFA)/H_2O (4:1) at 0 °C to provide **5**, and subsequent treatment of **5** with K_2CO_3 in MeOH at room temperature led to **6** in 72% yield over this three step sequence. We also noticed that the debenzylation reaction produced different results when we used a fresh batch of Pd/C catalyst from the same vendor. Thus, under the same reaction conditions with the new batch of Pd/C catalyst, both the benzyl groups and the triethylsilyl groups were removed to provide **5** in 74% yield. Moreover, elongated reaction time also reduced the C3 carbonyl group of quillaic acid domain based on ^1H NMR and mass spectroscopy analysis, which was not observed in the earlier synthesis of the QS-21 natural products and analogs.[15,16,29]

With **5** and **6** in hand, we evaluated their adjuvant activity and compared it with the known saponin adjuvant GPI-0100, which is a semisynthetic sapoinin mixture prepared from commercially available Quil A, a QS tree bark extract mixture that contains QS-7 and −21.[30,31] GPI-0100 retains Quil A's capacity to potentiate humoral and T-cell immunity with the production of antigen-specific CTL. Moveover, GPI-0100 has much reduced toxicity compared with the QS natural products, including QS-21. It has been frequently used in various preclinical studies.[32]

In our first set of experiments, we evaluated the effectiveness of **5** and **6** in augmenting immune responses to recombinant hemagglutinin B (rHagB), which is a recombinant, nonfimbrial adhesion hemagglutinin B from *Porphyromonas gingivalis*, an etiologic agent of periodontal disease.[32–34] Previous studies have demonstrated the effectiveness of rHagB in inducing a protective immune response against *P. gingivalis*-induced alveolar bone loss in an experimental animal model.[35] Groups of female BALB/c mice (8–10 weeks of age, six per group) were immunized via a subcutaneous (s.c.) route with rHagB (35 μg) antigen alone or with GPI-0100 or different synthetic adjuvants on days 0, 14, and 28. We used GPI-0100, **5**, or **6** at the dosage of 1000020μg. Prior to each immunization and on day 42 post the last immunization, mice were weighed and then serum was collected from each mouse and

analyzed for antirHagB activity using an enzyme-linked immunosorbent assay (ELISA). No sign of toxicity was observed in all the mice based on weight monitoring (see the Supporting Information).

A serum immunoglobulin G (IgG) anti-rHagB response was detected in all immunized mice by week 2 after the initial immunization (Figure 3). The magnitude of the response continued to increase following the second immunization. As expected, the serum IgG anti-rHagB antibody responses induced with rHagB + GPI-0100 were significantly higher than those induced with rHagB alone at weeks 2 and 4 (P <0.001). However, unlike in our earlier studies, the two groups did not show a significant difference at week 6, presumably due to the change of rHagB dose from 20 to 35 μg.[15,16] QS-7 analog **5** also potentiated a significantly higher IgG response to rHagB than antigen alone at weeks 2 and 4 (P < 0.001). In addition, a significantly higher response was noticed at week 6 (P < 0.05) in mice receiving **5** than in mice receiving antigen alone. Furthermore, a significant higher IgG response was observed at week 4 (P < 0.05) in mice immunized with **5** than in mice immunized with GPI-0100. On the other hand, although QS-7 analog **6** also potentiated a higher serum antirHagB IgG activity than mice receiving antigen alone, a significant difference was observed at week 4 (P < 0.05) between the two groups. In addition, significantly lower IgG responses were seen with analog **6** than those seen with GPI-0100 at weeks 2 (P < 0.001) and 4 (P < 0.05), as well as those seen with analog **5** at weeks 2 (P < 0.01), 4 (P < 0.001), and 6 (P < 0.05). These results indicate that QS-7 analog **5** was comparable to GPI-0100 in potentiating a serum IgG response to rHagB following systemic immunization, whereas analog **6** was less effective than GPI-0100 or analog **5** in this regard.

Since serum IgG subclass distribution is indicative of Th1- or Th2-biased immunity, we analyzed the IgG subclass antibody responses induced by different adjuvants. QS-7 analog **5** and GPI-0100 showed significantly higher serum IgG1 anti-rHagB responses than those induced by rHagB alone at weeks 2 (P < 0.001) and 4 (P < 0.001) (Figure 4A). In addition, adjuvant **5** also showed higher IgG1 activity than GPI-0100 at week 4 (P < 0.01). The levels of serum IgG1 antibody activity induced by analog **6** were significantly higher than those induced by antigen alone at weeks 2 (P < 0.05) and 4 (P < 0.01); however, these responses were lower than those observed in mice receiving GPI-0100 at week 2 (P < 0.001) or analog **5** at weeks 2 (P < 0.001) and 4 (P < 0.001).

In terms of IgG2a responses, mice immunized with rHagB + GPI-0100 showed significantly higher activity than that of rHagB alone at weeks 2 (P < 0 0.001), 4 (P < 0.05), and 6 (P <0.05), while there was no significant difference between GPI-0100 and analog **5** (Figure 4B). Mice immunized with rHagB + **6** did not show significant differences in the IgG2a activity from mice immunized with rHagB alone but show lower activity than mice immunized with rHagB + GPI-0100 at weeks 2 (P < 0 0.001), 4 (P < 0.05), and 6 (P < 0.05) and also mice immunized with rHagB + **5** at weeks 4 (P < 0.01) and 6 (P < 0.05).

Further analysis of the IgG2a/IgG1 ratio of the anti-rHagB responses indicated that the antigen alone or with adjuvant **6** selectively induced a Th2-like response by preferentially potentiating serum IgG1 antibody responses (Table 1). However, similar to GPI-0100, analog 5 potentiated both Th1- and Th2-like responses to rHagB, with a shift toward an

enhanced Th1-like response compared to rHagB alone. These results demonstrated that **5** and **6** had significantly different adjuvant activity profiles ($P < 0.05$), which suggests that the acetyl groups of **5** on its fucopyranosyl unit at C28 of quillaic acid have a significant impact on its ability to induce a IgG2a response.

We then focused on **5** and evaluated its adjuvant activity by formulating it with another antigen, i.e., the recombinant heat shock protein DnaK from *Francisella tularensis*, the cause of tularemia and a category A select agent. We have immunologically characterized DnaK.[36] It is lowly immunogenic if given alone but induces good responses when given with GPI-0100 by the intranasal (i.n.) route and provides protection against a lethal respiratory challenge with *F. tularensis*.[37] Thus, we immunized groups of female BALB/c mice (8–10 weeks of age, six per group) via the s.c. route with Dnak (10 μg) antigen alone or with GPI-0100 or **5** on days 0, 14, and 28, using the same aforementioned protocol of rHagB. In this set of experiments, two doses of GPI-0100 (50 and 100 μg) or **5** (50 and 100 μg) were used to assess the dose-dependent adjuvant activities.

A serum IgG response was detected in all mice by week 2 after the initial immunization, and the magnitude of the response continued to increase in all groups of mice. At week 6, IgG anti-Dnak antibody responses induced with Dnak + adjuvant (at different dose) were significantly higher ($P < 0.001$) than those induced with Dnak alone (Figure 5). The group of GPI-0100 (100 μg) and the group of adjuvant **5** (100 μg) did not show a significant difference between each other in potentiating the serum IgG anti-Dnak responses and neither did these two adjuvants at a 50 μg dose. In evaluating dose dependence, the group with GPI-0100 at 100 μg showed significantly higher IgG responses ($P < 0.05$) than the group at a lower dose of 50 μg while adjuvant **5** did not show a significant difference in IgG responses at doses of 100 or 50 μg.

We also analyzed the IgG subclass antibody responses (Figure 6). At week 6, there showed significantly higher levels of IgG1 antibody activity for mice immunized with Dnak + GPI-0100 (100 μg) ($P < 0.001$), Dnak + GPI-0100 (50 μg) ($P < 0.001$), Dnak + **5** (100 μg) ($P < 0.001$), or Dnak + **5** (50 μg) ($P < 0.01$) than mice receiving antigen alone. All groups with different doses of adjuvants showed similar IgG1 activity. In terms of IgG2a responses, the groups of mice immunized with GPI-0100 (100 μg) ($P < 0.05$ at weeks 4 and 6) or **5** (100 μg) ($P < 0.01$ at week 4, $P < 0.001$ at week 6) showed significantly higher IgG2a activity than the group immunized with the antigen alone. There also showed dose dependence of **5**; mice received **5** at a 100 μg dose induced higher IgG2a than those at a 50 μg dose at weeks 4 and 6 ($P < 0.05$). The IgG2a/IgG1 ratio of the anti-Dnak antibody responses indicated that Dnak alone preferentially induced IgG1 antibody responses (Table 2). However, adjuvant 5 showed a significantly higher IgG2a/IgG1 ratio than the group with the antigen alone ($P < 0.01$), suggesting that it potentiated both IgG1 and IgG2a responses to Dnak with a shift toward a mixed Th1- and Th2-like response, which is consistent with our observations from immunization with rHagB + **5**. No sign of toxicity was observed in all the mice based on weight monitoring (see the Supporting Information).

CONCLUSION

We synthesized QS-7 analogs **5** and **6**. The challenging pentasaccharide portion of the molecules was synthesized by using a two-stage allyl-glycoside-donor-activation chemical glycosylation approach, which only employs allyl glycoside building blocks, i.e., **7**–**11**. We evaluated the QS-7 analogs **5** and **6** in formulation with the protein antigen rHagB against the positive control GPI-0100, and the results show that **5** and **6** have significantly different adjuvant activity profiles, especially in boosting IgG2a responses. In the formulation of **5** with the other protein antigen Dnak, we confirmed the comparable adjuvant activity profiles between adjuvant **5** and GPI-0100. Moreover, adjuvant **5** retained its adjuvant activity with its dose reducing from 100 to 50 μg. These results suggest that the 3- and/or 4-O acetyl groups of the fucosyl unit may play an important role in tuning the adjuvanticity of the QS-7 analogs, and compound 5 can serve as a structurally defined synthetic adjuvant when a mixed Th1/Th2 immune response is desired and as a molecular probe for mechanistic studies.

EXPERIMENTAL SECTION

Chemistry.

General.—Organic solutions were concentrated by rotary evaporation at ca. 12 Torr. Flash column chromatography was performed by employing 230–400 mesh silica gel. Thin-layer chromatography was performed using glass plates precoated to a depth of 0.25 mm with 230–400 mesh silica gel impregnated with a fluorescent indicator (254 nm). Infrared (IR) data are presented as frequency of absorption (cm^{-1}). Proton and carbon-13 nuclear magnetic resonance (^{1}H NMR or ^{13}C NMR) spectra were recorded on 400, 700, and 850 MHz NMR spectrometers; chemical shifts are expressed in parts per million (δ scale) downfield from tetramethylsilane and are referenced to residual protium in the NMR solvent ($CHCl_3$: $\delta = 7.26$). Data are presented as follows: chemical shift, multiplicity (s = singlet, d = doublet, t = triplet, q = quartet, m = multiplet and/or multiple resonances, AB = AB quartet), coupling constant in Hertz (Hz), integration. Anhydrous solvents were used without distillation. Solvents for workup and column chromatography were obtained from commercial vendors and used without further purification. The purity of all synthetic intermediates and products was measured by ^{1}H NMR and was found to be ≥90%. The purity of all compounds evaluated in the immunological study was determined by a combination of high performance liquid chromatography (HPLC), high resolution mass spectrometry (HRMS), and 1H NMR and found to be ≥95%. All *in vivo* studies were performed in accordance with local International Animal Care and Use Committee (IACUC) guidelines.

Preparation of 5.

Compound 14 (15.0 mg, 4.0 μmol) and Pd/C (5.0 mg, 10% w/w, new batch) were mixed in 1.0 mL of tetrahydrofuran (THF)/MeOH (1:1). The reaction mixture was shaken under H_2 atmosphere (55 psi) for 6.5 h, filtered through a Celite plug, and concentrated. The crude product was then purified with RP HPLC by using a semiprep 250 × 10 mm, 5 μm C18 column and H_2O/acetonitrile (MeCN) gradients (90–10% H_2O over 30 min with 3 mL/min

flow rate). The desired product had a retention time of 26 min, and the fraction was concentrated on a rotary evaporator at room temperature to remove MeCN; the remaining water was then removed on a lyophilizer to provide final product **5** (5.2 mg, 74%) as a white solid. ^{1}H NMR (700 MHz, CD_3OD) (characteristic protons) δ 9.48 (s, 1H), 5.52 (d, J = 8.3 Hz, 1H), 5.37 (s, 1H), 5.23 (s, 1H), 5.14 (d, J = 9.8 Hz, 1H), 5.04 (s, 1H), 4.82 (d, J = 6.7 Hz, 1H), 4.73 (d, J = 9.0 Hz, 1H),4.64 (d, J = 8.3 Hz, 1H), 4.60 (d, J = 7.5 Hz, 1H), 4.54–4.51 (m, 2H), 4.48 (s, 1H), 2.95 (d, J = 14.7 Hz, 1H), 2.28 (t, J =12.7 Hz, 1H), 2.21 (s, 3H), 2.09 (s, 3H), 0.76 (s, 3H); ^{13}C NMR (214 MHz, CD_3OD) δ 210.8, 176.1, 172.2, 171.3, 142.9, 122.2, 117.4, 116.1, 104.4, 103.9, 103.4, 103.3, 103.0, 102.3, 100.2, 93.1, 86.6, 85.1, 84.6, 81.2, 77.7, 76.6, 76.4, 76.2, 76.1,75.4, 74.9, 94.8, 93.8, 73.7, 73.6, 73.4, 73.1, 72.1, 71.9, 70.9,70.3, 69.9, 69.5, 69.4, 69.1, 68.5, 67.9, 65.5, 65.0, 61.0, 60.3,55.2, 49.0, 41.4, 40.9, 39.7, 37.8, 35.6, 35.0, 32.3, 32.0, 30.3,29.9, 25.9, 24.3, 23.6, 23.1, 21.0, 20.3, 19.8, 19.4, 17.4, 16.7,15.1, 14.8, 9.6; HRMS (ESI-TOF) m/z: $[M + H]^+$ calcd for $C_{79}H_{123}O_{43}$, 1759.7438; found, 1759.7372.

Preparation of 6.

Compound **14** (15.0 mg, 4.0 μmol) and Pd/C (6.0 mg, 10% w/w) were mixed in 1.0 mL of THF/MeOH (1:1). The reaction mixture was shaken under H_2 atmosphere (55 psi) for 18 h, filtered through a Celite plug, and concentrated. The crude product was then cooled 0 °C and treated with 0.5 mL of TFA/water (1:1, v/v) precooled to 0 °C. The reaction solution was stirred at 0 °C for 40 min and then concentrated to dryness at 0 °C. To the residue were added 0.5 mL of MeOH and K_2CO_3 (20 mg, 0.14 mmol). The reaction mixture was stirred at room temperature for 12 h. The white suspension was centrifuged, and the clear solution was acidified with AcOH, concentrated, and purified with RP HPLC by using a semiprep 250 × 10 mm, 5 μm C18 column and H_2O/MeCN gradients (90–10% H_2O over 30 min with 3 mL/min flow rate). The desired product had a retention time of 16 min, and the fraction was concentrated on a rotary evaporator at room temperature to remove MeCN; the remaining water was then removed on a lyophilizer to provide final product **6** (4.8 mg, 72%) as a white solid. ^{1}H NMR (700 MHz, CD_3OD) (characteristic protons) δ 9.50 (s, 1H), 5.34 (s, 2H), 5.30 (d, J = 8.7 Hz, 1H), 4.75 (d, J = 8.0 Hz, 1H),4.61 (d, J = 7.3 Hz, 1H), 4.56 (d, J = 8.0 Hz, 1H), 4.54 (d, J =8.0 Hz, 1H), 4.51–4.50 (m, 2H), 4.28 (s, 1H), 2.97 (d, J =14.9 Hz, 1H), 2.33 (t, J = 12.6 Hz, 1H), 1.42 (s, 3H), 1.31 (d, J = 6.7 Hz, 3H), 1.24 (d, J = 6.1 Hz, 3H), 1.03 (s, 3H), 0.98 (s, 3H), 0.91 (s, 3H), 0.79 (s, 3H); HRMS (ESI-TOF) m/z: $[M + Na]^+$ calcd for $C_{75}H_{118}NaO_{41}$, 1697.7046; found, 1697.7036.

Antigens.

Recombinant *Porphyromonas gingivalis* HagB was prepared as previously described.[32–34] Briefly, the hagB gene was cloned from *P. gingivalis* 381 into a pET vector with a lac promoter and histidine tag and expressed in *Escherichia coli* JM109 (kindly provided by Ann Progulske-Fox and Thomas Brown, University of Florida, Gainesville). Protein expression was induced following isopropyl-β-D-thiogalactopyranoside (IPTG) induction. rHagB was purified from the soluble fraction of the bacterial lysates by using a His-bind resin column, according to the manufacturer's instruction (Novagen, Madison, WI). The purity of rHagB was confirmed by silver staining and Western blot analysis using a rabbit anti-rHagB antibody. Recombinant *Francisella tularensis* DnaK was prepared as previously

described.[36–38] Briefly, the gene encoding DnaK (originally obtained from Anders Sjostedt, Umea University, Sweden) was cloned into the pET-23d vector (Novagen) and was used to transform *E. coli* strain BL21 (DE3) pLysS for protein expression (Novagen). Protein expression was induced following IPTG induction. DnaK was purified using a three-step purification procedure comprised of affinity, anion exchange, and size exclusion chromatography and has been shown to be free of endotoxin (LPS).[36,37] The concentrations of rHagB and Dnak were estimated by the bicinchoninic acid protein determination assay (Pierce, Rockford, IL), using bovine serum albumin (BSA) as the standard.

Mice and Immunization.

BALB/c mice used in this study were purchased from Frederick Cancer Research (Fredrick, MD) and maintained within an environmentally controlled, pathogen-free animal facility at the University of Alabama at Birmingham (UAB). To assess the adjuvant activity of the QS saponin-based immune adjuvants, groups of female mice (8–10 weeks of age; 6 mice per group) were immunized by the subcutaneous (s.c.) route with rHagB (35 μg) or DnaK (10 μg) alone or with antigen plus proper adjuvant such as GPI-0100 (100 μg) or synthetic adjuvant 7 (100 or 50 μg) on days 0, 14, and 28. Prior to each immunization and at 2 weeks post last immunization, mice were weighed and blood samples were collected from the lateral tail vein by using heparinized capillary pipettes. The serum was obtained after centrifugation and stored at −20 °C until assayed. All studies were performed according to National Institutes of Health guidelines, and protocols were approved by the UAB Institutional Animal Care and Use Committee.

Evaluation of Antibody Responses.

The levels of specific serum IgG and IgG subclasses against rHagB or Dnak in each group were determined by an enzyme-linked immunosorbent assay (ELISA). Maxisorpmicrotiter plates (NUNC International, Roskilde, Denmark) were coated with rHagB (1 μg/mL), Dnak (1 μg/mL), or optimal amounts of goat antimouse IgG, IgG1, or IgG2a (Southern Biotechnology Associates, Inc., Birmingham, AL) in borate buffer saline (BBS; 100 mM NaCl, 50 mM boric acid, 1.2 mM $Na_2B_4O_7$, pH 8.2) at 4 °C overnight. Plates were blocked with 1% bovine serum albumin (BSA) and 0.02% sodium azide in BBS for 2 h at room temperature. Serial 2-fold dilutions of serum samples were added in duplicate to the plates. To generate standard curves, serial dilutions of a mouse immunoglobulin reference serum (MP Biomedicals, Solon, OH) were added to two rows of wells in each plate that had been coated with the appropriate antimouse IgG or IgG subclass reagent. After incubation (overnight at 4 °C) and washing of the plates, horseradish peroxidase-conjugated goat antimouse IgG or IgG subclass antibody (Southern Biotechnology Associates, Inc.) was added to the appropriate wells. After 4 h of incubation at room temperature, plates were washed and developed by *o*-phenylenediamine substrate with hydrogen peroxide. Color development was recorded at 490 nm. The concentrations of antibodies were determined by interpolation on standard curves generated by using the mouse immunoglobulin reference serum and constructed by a computer program based on four-parameter logistic algorithms (Softmax/Molecular Devices Corp., Menlo Park, CA).

Statistical Analysis.

Statistical significance in antibody responses and body weights between groups was evaluated by ANOVA and the Tukey multiple-comparisons test using GraphPad Prism 8.0.1. Differences were considered significant at a P value < 0.05.

Supplementary Material

Refer to Web version on PubMed Central for supplementary material.

ACKNOWLEDGMENTS

We thank the NIH (AI099407 and GM120159 to P.W.) for financial support.

ABBREVIATIONS

QS	Quillaja saponaria
Th	T helper cells
FDA	U.S. Food and Drug Administration
GSK	GlaxoSmithKline
CTL	cytotoxic T cell
CD8	cluster of differentiation 8
Ac	acetyl
Ir	iridium
COD	cyclooctadiene
P	phosphine
Me	methyl
Ph	phenyl
F	fluoro
NIS	*N*-iodosuccinimide
TfOH	triflic acid
TFA	trifluoroacetic acid
NMR	nuclear magnetic resonance
ppm	parts per million
rHagB	recombinant hemagglutinin B
ELISA	enzyme-linked immunosorbent assay

IgG	immunoglobulin G
Hz	Hertz
THF	tetrahydrofuran
MeCN	acetonitrile
HPLC	high performance liquid chromatography
HRMS	high resolution mass spectrometry
IACUC	International Animal Care and Use Committee

REFERENCES

(1). Brito LA, and O'Hagan DT (2014) Designing and building the next generation of improved vaccine adjuvants. J. Controlled Release 190, 563–579.

(2). Brunner R, Jensen-Jarolim E, and Pali-Scholl I (2010) The ABC of clinical and experimental adjuvants–a brief overview. Immunol. Lett 128 (1), 29–35. [PubMed: 19895847]

(3). Di Pasquale A, Preiss S, Tavares Da Silva F, and Garcon N (2015) Vaccine Adjuvants: from 1920 to 2015 and Beyond. Vaccines (Basel, Switz.) 3 (2), 320–343.

(4). Didierlaurent AM, Laupeze B, Di Pasquale A, Hergli N, Collignon C, and Garcon N (2017) Adjuvant system AS01: helping to overcome the challenges of modern vaccines. Expert Rev. Vaccines 16 (1), 55–63. [PubMed: 27448771]

(5). Kensil CR (1996) Saponins as vaccine adjuvants. Crit. Rev. Ther. Drug Carrier Syst 13, 1–55. [PubMed: 8853958]

(6). Kensil CR, Liu G, Anderson C, and Storey J (2005) Effects of QS-21 on innate and adaptive immune responses In Vaccine Adjuvants: Immunological and Clinical Principles (Hackett CJ, and Harn DAJ, Eds.), pp 221–234, Humana Press Inc., Totowa, NJ, DOI: 10.1007/978-1-59259-970-7.

(7). Garcon N, and Van Mechelen M (2011) Recent clinical experience with vaccines using MPL- and QS-21-containing adjuvant systems. Expert Rev. Vaccines 10 (4), 471–486. [PubMed: 21506645]

(8). Ragupathi G, Gardner JR, Livingston PO, and Gin DY (2011) Natural and synthetic saponin adjuvant QS-21 for vaccines against cancer. Expert Rev. Vaccines 10, 463–470. [PubMed: 21506644]

(9). Adams MM, Damani P, Perl NR, Won A, Hong F, Livingston PO, Ragupathi G, and Gin DY (2010) Design and synthesis of potent Quillaja saponin vaccine adjuvants. J. Am. Chem. Soc 132, 1939–1945. [PubMed: 20088518]

(10). Chea EK, Fernandez-Tejada A, Damani P, Adams MM, Gardner JR, Livingston PO, Ragupathi G, and Gin DY (2012) Synthesis and preclinical evaluation of QS-21 variants leading to simplified vaccine adjuvants and mechanistic probes. J. Am. Chem. Soc 134 (32), 13448–13457. [PubMed: 22866694]

(11). Fernández-Tejada A, Chea EK, George C, Gardner JR, Livingston PO, Ragupathi G, Tan DS, and Gin DY (2014) Design, synthesis, and immunologic evaluation of vaccine adjuvant conjugates based on QS-21 and tucaresol. Bioorg. Med. Chem 22, 5917–5923. [PubMed: 25284254]

(12). Fernéndez-Tejada A, Chea EK, George C, Pillarsetty N, Gardner JR, Livingston PO, Ragupathi G, Lewis JS, Tan DS, and Gin DY (2014) Development of a minimal saponin vaccine adjuvant based on QS-21. Nat. Chem 6, 635–643. [PubMed: 24950335]

(13). Ragupathi G, Damani P, Deng K, Adams MM, Hang J, George C, Livingston PO, and Gin DY (2010) Preclinical evaluation of the synthetic adjuvant SQS-21 and its constituent isomeric saponins. Vaccine 28 (26), 4260–4267. [PubMed: 20450868]

(14). Walkowicz WE, Fernandez-Tejada A, George C, Corzana F, Jimenez-Barbero J, Ragupathi G, Tan DS, and Gin DY (2016) Quillaja saponin variants with central glycosidic linkage

modifications exhibit distinct conformations and adjuvant activities. Chem. Sci 7, 2371–2380. [PubMed: 27014435]

(15). Wang P, Dai Q, Thogaripally P, Zhang P, and Michalek SM (2013) Synthesis of QS-21-based immunoadjuvants. J. Org. Chem 78, 11525–11534. [PubMed: 24147602]

(16). Wang P, Devalankar DA, Dai Q, Zhang P, and Michalek SM (2016) Synthesis and evaluation of QS-21-based immunoadju-vants with a terminal-functionalized side chain incorporated in the west wing trisaccharide. J. Org. Chem 81, 9560–9566. [PubMed: 27709937]

(17). Wang P,Škalamera Đ, Sui X, Zhang P, and Michalek SM (2019) Synthesis and evaluation of a QS-17/18-based vaccine adjuvant. J. Med. Chem 62, 1669–1676. [PubMed: 30656932]

(18). Kensil CR, Wu J-Y, Anderson CA, Wheeler DA, and Amsden J (1998) QS-21 and QS-7: Purified saponin adjuvants. Dev. Biol. Stand 92, 41–47. [PubMed: 9554258]

(19). Deng K, Adams MM, and Gin DY (2008) Synthesis and structure verification of the vaccine adjuvant QS-7-api. Synthetic access to homogeneous Quillaja saponaria immunostimulants. J. Am. Chem. Soc 130, 5860–5861. [PubMed: 18410100]

(20). Cleland J, Kensil CR, Lim A, Jacobsen NE, Basa L, Spellman M, Wheeler DA, Wu J-Y, and Powell MF (1996) Isomerization and formulation stability of the vaccine adjuvant QS-21. J. Pharm. Sci 85 (1), 22–28. [PubMed: 8926578]

(21). Marciani D (2015) Is fucose the answer to the immunomodulatory paradox of Quillaja saponins? Int. Immunopharmacol 29, 908–913. [PubMed: 26603552]

(22). Wang P, Haldar P, Wang Y, and Hu H (2007) Simple glycosylation of allyl glycosides. J. Org. Chem 72, 5870–5873. [PubMed: 17580902]

(23). Wang Y, Liang X, and Wang P (2011) Concise synthesis of Bacillus anthracis exosporium tetrasaccharide via two-stage activation of allyl glycosyl donor strategy. Tetrahedron Lett. 52, 3912–3915.

(24). Wang Y, Zhang X, and Wang P (2010) Facile glycosylation strategy with two-stage activation of allyl glycosyl donors. Application to concise synthesis of Shigella flexneri serotype Y O-antigen. Org. Biomol. Chem 8, 4322–4328. [PubMed: 20683518]

(25). Yang H, and Wang P (2013) Mechanistic study of glycosylation using a prop-1-enyl donor. J. Org. Chem 78, 1858–1863. [PubMed: 23106235]

(26). Baudry D, Ephritikhine M, and Felkin HJ (1978) Isomerization of allyl ethers catalyzed by the cationic iridium complex [Ir(cyclo-octa-1,5-diene)(PMePh2)2]PF6. A highly stereoselective route to trans-propenyl ethers. J. Chem. Soc., Chem. Commun, 694–695.

(27). Oltvoort JJ, Van Boeckel CAA, De Koning JH, and Van Boom JH (1981) Use of the cationic iridium complex 1,5-cyclooctadienebis[methyldiphenylphosphine]iridium hexafluorophos-phate in carbohydrate chemistry: smooth isomerization of allyl ethers to 1-propenyl ethers. Synthesis 1981, 305–308.

(28). Gigg J, and Gigg R (1966) Allyl ether as a protecting group in carbohydrate chemistry. J. Chem. Soc C 1, 82–86.

(29). Wang P, Kim Y-J, Navarro-Villalobos M, Rohde BD, and Gin DY (2005) Synthesis of the potent immunostimulatory adjuvant QS-21A. J. Am. Chem. Soc 127, 3256–3257. [PubMed: 15755124]

(30). Marciani D, Press JB, Reynolds RC, Pathak AK, Pathak V, Gundy LE, Farmer JT, Koratich MS, and May RD (2000) Development of semisynthetic triterpenoid saponin derivatives with immune stimulating activity. Vaccine 18, 3141–3151. [PubMed: 10856794]

(31). Marciani DJ, Reynolds RC, Pathak AK, Finley-Woodman K, and May RD (2003) Fractionation, structural studies, and immunological characterization of the semi-synthetic Quillaja saponins derivative GPI-0100. Vaccine 21 (25–26), 3961–3971. [PubMed: 12922132]

(32). Zhang P, Yang Q-B, Marciani DJ, Martin M, Clements JD, Michalek SM, and Katz J (2003) Effectiveness of the quillaja saponin semi-synthetic analog GPI-0100 in potentiating mucosal and systemic responses to recombinant HagB from Porphyromonas gingivalis. Vaccine 21 (27–30), 4459–4471. [PubMed: 14505929]

(33). Zhang P, Martin M, Yang Q-B, Michalek SM, and Katz J (2004) Role of B7 costimulatory molecules in immune responses and T-helper cell differentiation to recombinant HagB from Prophyromonas gingivalis. Infect. Immun 72, 637–644. [PubMed: 14742503]

(34). Zhang P, Martin M, Michalek SM, and Katz J (2005) Role of mitogen-activated protein kinases and NF-&B in the regulation of pro- and anti-inflammatory cytokines by Porphyromonas gingivalis Hemagglutinin B. Infect. Immun 73, 3990–3998. [PubMed: 15972486]

(35). Katz J, Black KP, and Michalek SM (1999) Host responses to recombinant hemagglutinin B of Porphyromonas gingivalis in an experimental rat model. Infect. Immun 67, 4352–4359. [PubMed: 10456874]

(36). Ashtekar AR, Zhang P, Katz J, Deivanayagam CCS, Rallabhandi P, Vogel SN, and Michalek SM (2008) TLR4-mediated activation of dendritic cells by the heat shock protein DnaK from Francisella tularensis. J. Leukocyte Biol 84, 1434–1446. [PubMed: 18708593]

(37). Ashtekar AR, Katz J, Xu Q, and Michalek SM (2012) A mucosal subunit vaccine protects against lethal respiratory infection with Francisella tularensis LVS. PLoS One 7 (11), e50460. [PubMed: 23209745]

(38). Thakran S, Li H, Lavine CL, Miller MA, Bina JE, Bina XR, and Re F (2008) Identification of Francisella tularensis lipoproteins that stimulate the toll-like receptor (TLR) 2/TLR1 heterodimer. J. Biol. Chem 283 (7), 3751–3760. [PubMed: 18079113]

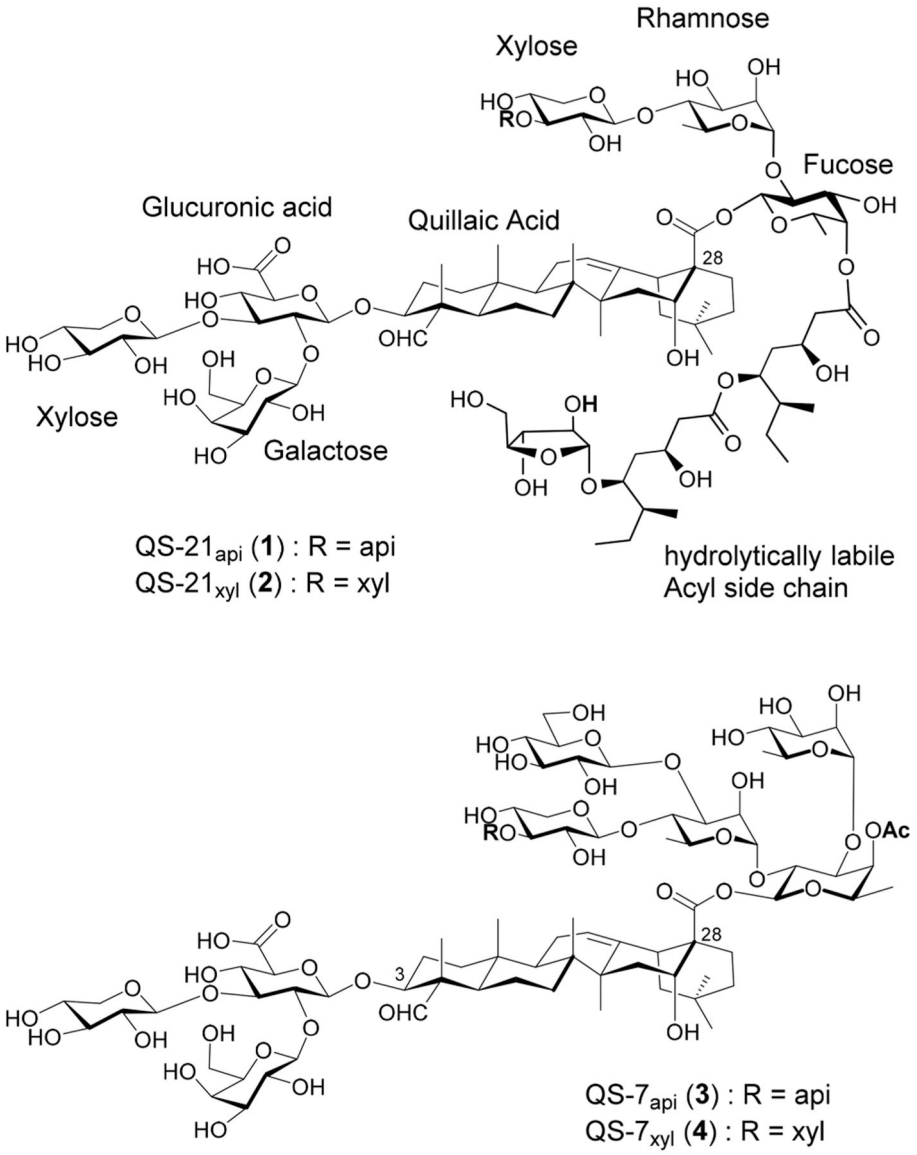

Figure 1.
Natural saponins from *Quillaja saponaria* Molina bark.

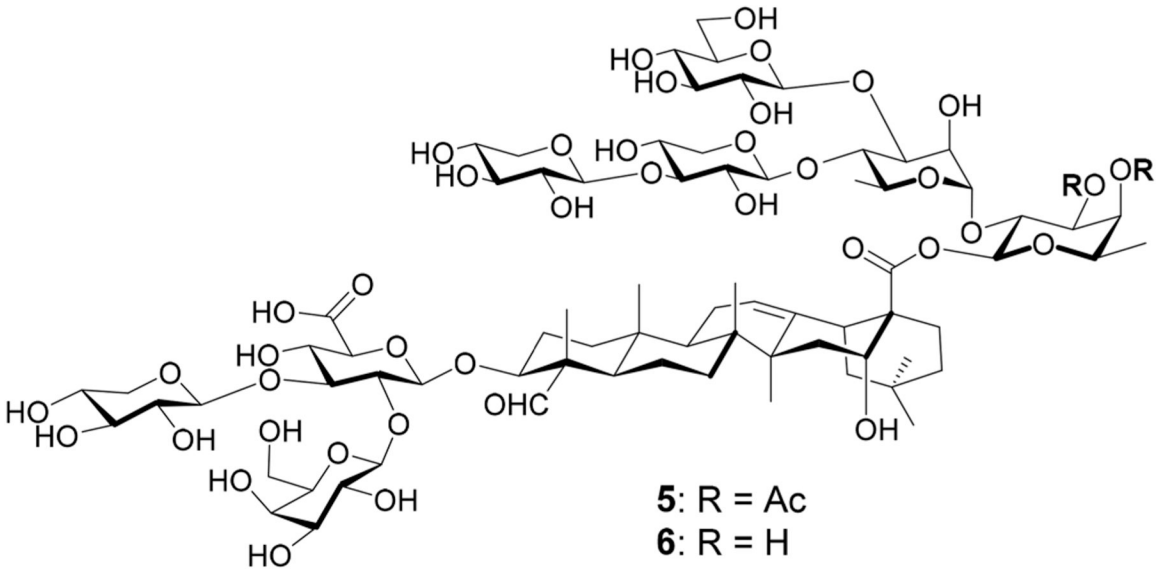

Figure 2.
QS-7 analogs **5** and **6**.

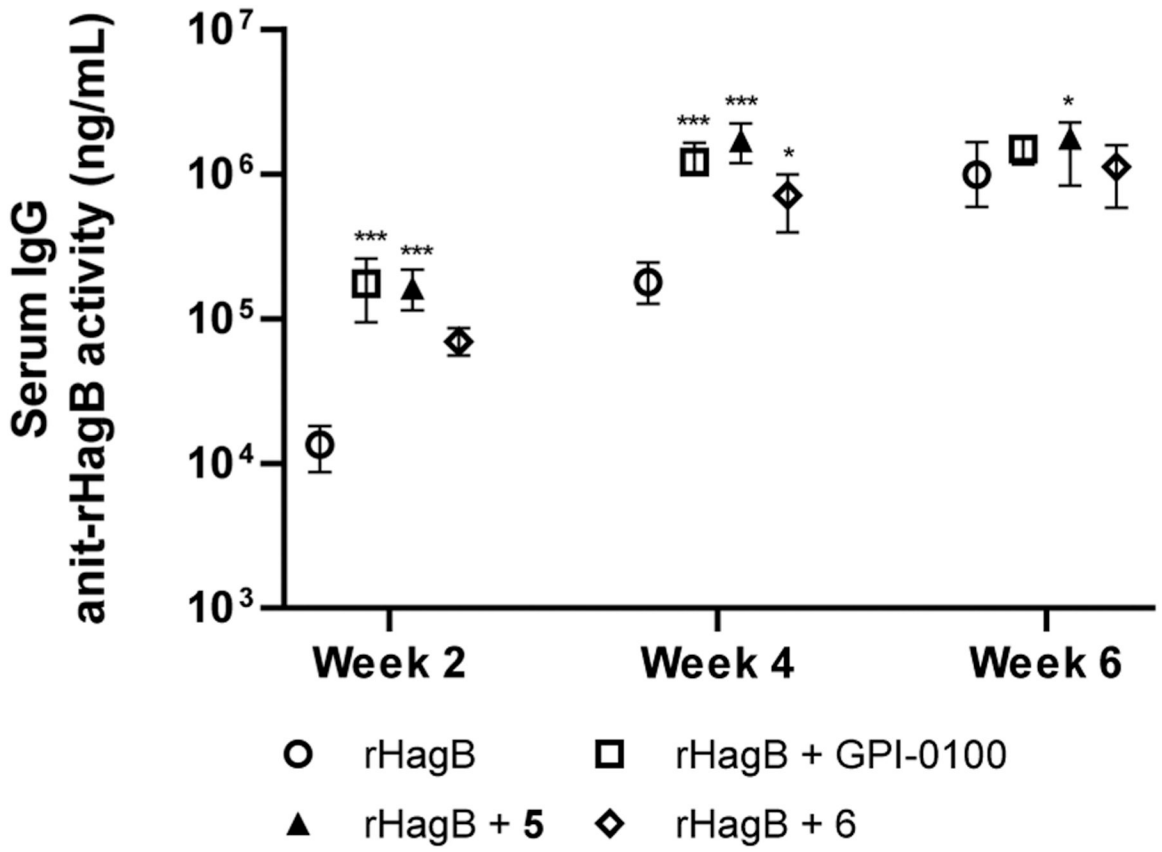

Figure 3.

Serum IgG anti-rHagB activity at weeks 2, 4, and 6. Data are expressed as the mean with the range. Statistical significance compared to no-adjuvant control group at $*P < 0.05$, $**P < 0.01$, and $***P < 0.001$.

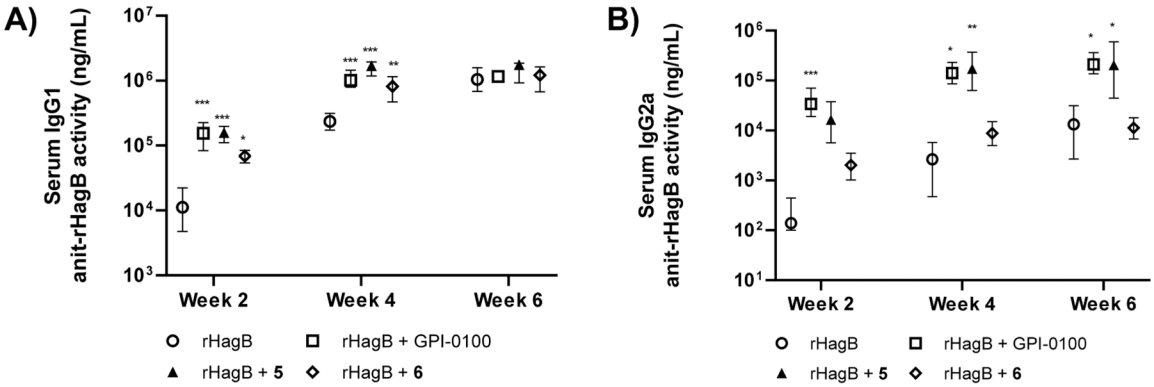

Figure 4.

Serum IgG1 (A) and IgG2a (B) anti-rHagB activities at weeks 2, 4, and 6. Data are expressed as the mean with the range. Statistical significance compared to no-adjuvant control group at $*P < 0.05$, $**P < 0.01$, and $***P < 0.001$.

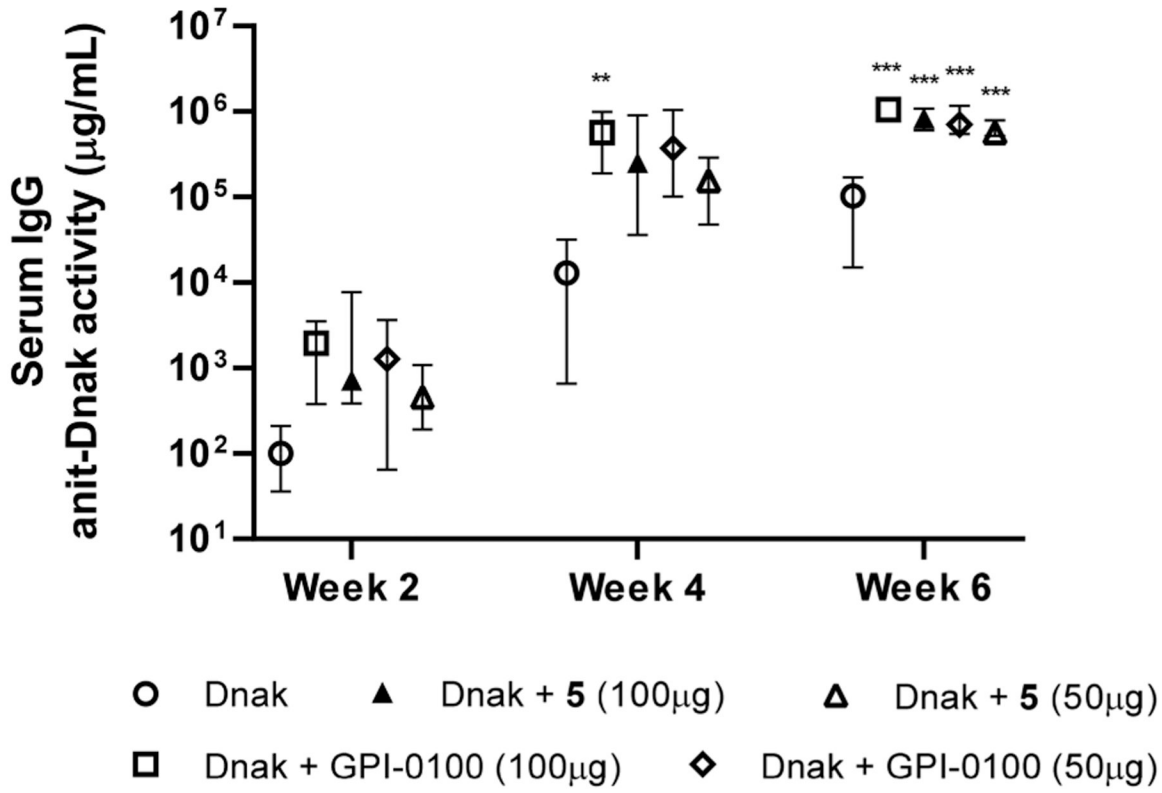

Figure 5.

Serum IgG anti-Dnak activity at weeks 2, 4, and 6. Data are expressed as the mean with the range. Statistical significance compared to no-adjuvant control at $*P < 0.05$, $**P < 0.01$, and $***P < 0.001$.

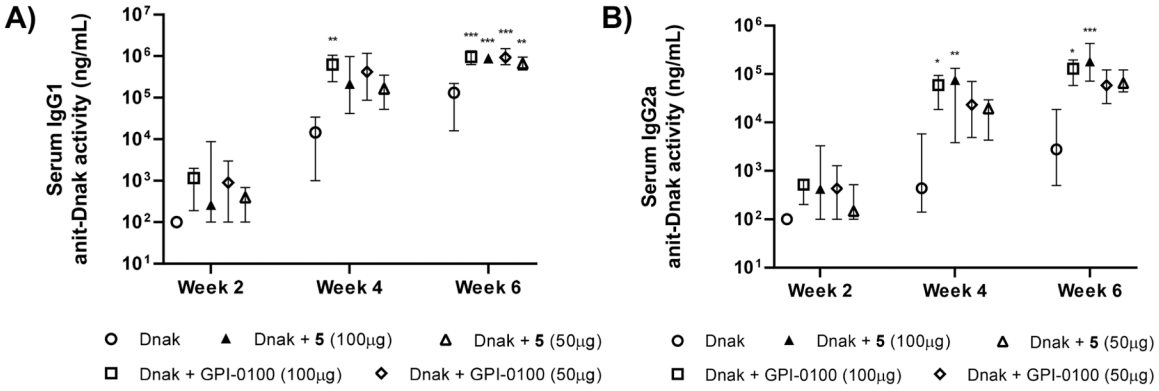

Figure 6.

Serum IgG1 (A) and IgG2a (B) anti-Dnak activities at weeks 2, 4, and 6. Data are expressed as the mean with the range. Statistical significance compared to no-adjuvant control at $*P < 0.05$, $**P < 0.01$, and $***P < 0.001$.

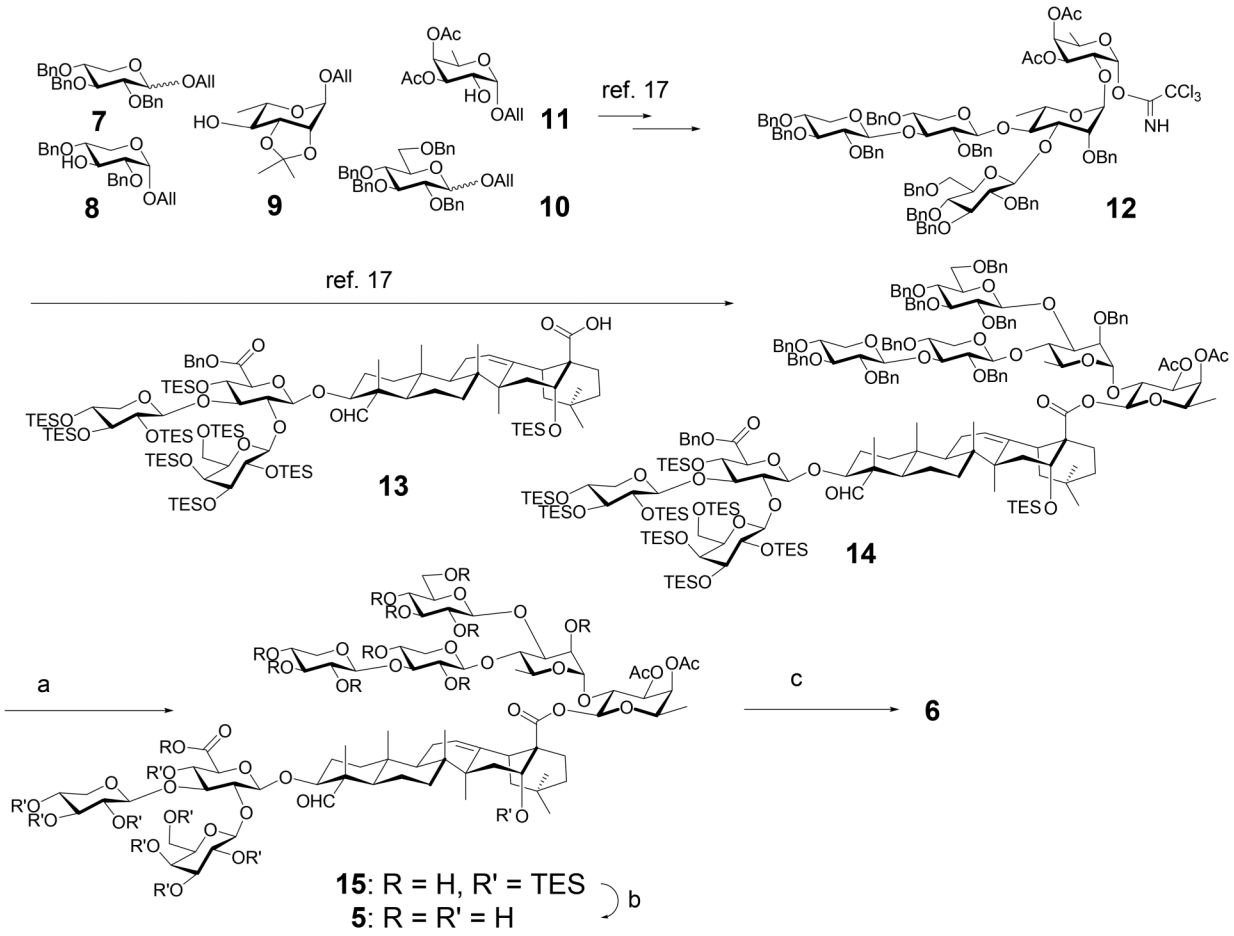

Scheme 1.

Synthesis of QS-7 Analog[a]

[a]Reagents and conditions: (a) Pd/C, H_2 (55 psi); (b) TFA/H_2O (4:1), 0 °C; (c) K_2CO_3, MeOH, 23 °C, 72% over three steps.

Table 1.

Serum IgG Subclass Anti-rHagB Activity at Week 6[a]

entry	adjuvant	IgG1 (μg/mL)	IgG2a (μg/mL)	IgG2a/IgG1
1	none	1090 ± 140	16 ± 5	0.014 ± 0.003
2	GPI-0100	1221 ± 80	231 ± 33	0.192 ± 0.031**
3	**5**	1605 ± 142	238 ± 86	0.142 ± 0.048*
4	**6**	1219 ± 147	11 ± 2	0.010 ± 0.001

[a]Values are expressed as mean ± SEM.

Statistical significance compared with no-adjuvant control group:

*$P < 0.05$,

**$P < 0.01$, and

***$P < 0.001$.

Table 2.

Serum IgG Subclass Anti-Dnak Activity at Week 6[a]

entry	adjuvant	IgG1 (μg/mL)	IgG2a (μg/mL)	IgG2a/IgG1
1	none	125 ± 27	5 ± 3	0.041 ± 0.017
2	GPI-0100 (100 μg)	993 ± 104	127 ± 25	0.123 ± 0.014
3	**5** (100 μg)	894 ± 82	212 ± 52	0.264 ± 0.081**
4	GPI-0100 (50 μg)	933 ± 131	59 ± 16	0.062 ± 0.014
5	**5** (50 μg)	676 ± 70	79 ± 14	0.129 ± 0.032

[a]Values are expressed as mean ± SEM.

Statistical significance compared with no-adjuvant control group:

*$P < 0.05$,

**$P < 0.01$, and

***$P < 0.001$.